Vapor-liquid equilibria of CO_2 + C1-C5 alcohols from experiment and the COSMO-SAC model

Chieh-Ming Hsieh*, Thorsten Windmann, Jadran Vrabec

[a] Thermodynamics and Energy Technology, University of Paderborn, Paderborn, Germany

Abstract

The phase behavior of CO_2 + alcohols is crucial for the design and optimization of extraction processes that use these alcohols as co-solvents to increase the solubility of polar solutes in supercritical CO_2. In this study, the vapor-liquid equilibria (VLE) of CO_2 + 2,2-dimethyl-1-propanol are measured at 333.2 K and 353.2 K with a high pressure view cell technique based on the synthetic method. This completes the literature database for binary VLE of CO_2 with low mass alcohols up to pentanols. We further systematically investigate the prediction of all binary CO_2 + C1-C5 alcohols mixtures with the COSMO-SAC model. Qualitative predictions are obtained when the COSMO-SAC model is combined with the Peng-Robinson-Stryjek-Vera equation of state through the modified Huron-Vidal 1st-order or the Wong-Sandler mixing rule.

Keywords: Peng-Robinson-Stryjek-Vera equation of state, phase equilibrium prediction, COSMO-SAC, experiment, carbon dioxide, alcohols

*To whom correspondence should be addressed: Email hsiehcm@mail.upb.de

1. Introduction

Supercritical carbon dioxide ($ScCO_2$) has a wide variety of applications in chemical, food and pharmaceutical industries. For example, $ScCO_2$ is used as a solvent for the decaffeination of coffee beans, the extraction of natural flavors or as a reaction medium in polymer synthesis processes.[1-8] However, since $ScCO_2$ has a limited capability (even at high pressures) for the extraction of polar solutes,[2, 9] low molar mass alcohols are added as co-solvents for increasing their solubility.[3, 5] The fluid phase behavior of CO_2 + low molar mass alcohol mixtures is thus crucial for the design and optimization of extraction processes that contain these alcohols as co-solvents. To the best of our knowledge, vapor-liquid equilibrium (VLE) data for all CO_2 + C1-C5 alcohols are available in literature, except for CO_2 + 2,2-dimethyl-1-propanol (CAS number: 75-84-3). Therefore, the first goal of this study was to generate experimental VLE data for this system. The molecular structures of all 16 C1-C5 alcohols are illustrated in Figure 1. The vapor pressure of CO_2 + 2,2-dimethyl-1-propanol was measured at 333.2 K and 353.2 K with a high pressure view cell technique based on the synthetic method between 5.33 MPa and 12.8 MPa.

Thermodynamic properties of fluids and their mixtures, in particular phase equilibrium data, are crucial information for process design and optimization.[10, 11] Experimental measurements are still the most reliable route for generating such data, however, it is not feasible to measure data under all required conditions, because it is too time-consuming and costly. This particularly holds for newly synthesized compounds that are part of drug development in the pharmaceutical industry.[12, 13] CO_2 + alcohol systems have been studied intensively by experimental and theoretical works because of their potential for industrial applications.[14-17] For these systems, it

was found that it is a challenging task to predict phase equilibrium properties without input of any experimental mixture data.[17] Therefore, the predictive power of the COSMO-SAC model, which does not require any experimental mixture data as an input, was studied here.

Being a relatively new model for liquid mixtures, the COSMO-based methods (COSMO-RS[18, 19] or COSMO-SAC[20-22]), were developed in the past two decades. They rely on quantum chemistry calculations to determine the nonideality of liquid mixtures. This type of model does not suffer from the issue of missing parameters, such as group contribution methods, because it does not contain any species-dependent parameters. In preceding work, the COSMO-SAC model was revised and it was shown that it provides acceptable predictions both for VLE and liquid-liquid equilibria (LLE) of mixtures under sub-critical conditions.[20] For mixtures containing a supercritical component, a straightforward approach is to combine the COSMO-SAC model with a cubic equation of state (EOS), such as the Peng-Robinson (PR) EOS or its modified version by Stryjek and Vera (PRSV EOS,[23] through an excess Gibbs free energy G^{ex} based mixing rule, such as the modified Huron-Vidal 1st-order (MHV1) mixing rule[24] or the Wong-Sandler (WS) mixing rule.[25, 26] In several publications, this approach was assessed for these two mixing rules, because they are classical and are widely used in industrial applications.[27-34] Thus, the second goal of this study was to evaluate the predictive power for mixtures of type CO_2 + C1-C5 alcohols on the basis of these two mixing rules, i.e.: PRSV+MHV1+COSMOSAC and PRSV+WS+COSMOSAC. It has been shown that the accuracy of this approach can be improved significantly with the introduction of binary interaction parameters,[7] however this was not the focus of this study. Finally, a case study on drug solubility in CO_2 + ethanol mixtures is conducted to demonstrate a

potential application of these two approaches.

2. Materials and methods

2.1. Materials

2,2-dimethyl-1-propanol (purity ≥ 99%) was purchased from Sigma-Aldrich, Germany. Carbon dioxide (volume fraction 99.995%) was supplied by Air Liquide, Germany. All chemicals were used without further purification.

2.2. Experimental apparatus and procedure

The employed experimental setup is shown in Figure 2. It is a modification of an apparatus which was used for gas solubility measurements in prior work.[35] Compared to the original installation that was described in Ref.[35], an additional calibrated high pressure spindle press B was introduced to load the high pressure view cell with 2,2-dimethyl-1-propanol. To measure the temperature in the cell and in the high pressure pumps, calibrated platinum resistance thermometers (T1 to T4) with a basic resistance of 100 Ω (Pt100) were employed. The temperature measuring error was about ± 0.04 K. Calibrated pressure transducers P1 and P2 (model Super THE, Honeywell test & measurement, measuring ranges: 6.8 MPa for P1 and 20 MPa for P2), with an accuracy of 0.05 % of their respective full measuring ranges, were used to determine the pressure in the view cell and in the supply pipes.

At the beginning of the measurement procedure, the calibrated spindle press A was cooled down to about 298 K and filled with CO_2 from the gas bottle. Hereby, the spindle press was loaded completely with liquid CO_2. The spindle press B was loaded with 2,2-dimethyl-1-propanol from the reservoir via valve V1. Due to the fact that the melting temperature of 2,2-dimethyl-1-propanol is about 325 K at ambient pressure, it

was filled in its solid state into the reservoir and melted therein. Therefore, the climate chamber was heated up to 353 K. When the spindle press B was completely filled with liquid 2,2-dimethyl-1-propanol, valve V1 was closed and the desired quantity of 2,2-dimethyl-1-propanol was loaded into the heated view cell via valve TW-V1. Next, the climate chamber and the view cell were brought to the desired measurement temperature and liquid CO_2 was added to the view cell with the spindle press A until the CO_2 was completely solved in 2,2-dimethyl-1-propanol. A magnetic stirrer was used to enhance the mixing process, which was visually observed with an endoscope. Starting from a homogeneous liquid state, the pressure in the view cell was decreased via the spindle press A in very small steps, until the first bubbles appeared and thus the saturated liquid state was reached. At this state, the vapor pressure of the mixture was measured with the pressure transducer P2.

The input volumes of 2,2-dimethyl-1-propanol and CO_2 were obtained from correlation functions, determined via calibration of the spindle press, between number of turns and the associated volume change of the spindle press. To convert input volume to molar fraction is straightforward as describing in the following. Temperature, pressure and volume of spindle press were recorded before and after the input of compounds. The input mass of CO_2 could be determined from its input volume and the liquid density determined from the equation of state[36] with recorded temperature and pressure. The input mass of 2,2-dimethyl-1-propanol was calculated by using experimental liquid density.[37, 38] Once the input mass of the compounds is known, the molar fraction can be calculated straightforwardly.

2.3. Thermodynamic models

In this study, the accuracy of a combination of the PRSV EOS[23] and the

COSMO-SAC model[20] through two different mixing rules with respect to the prediction of VLE of CO_2 + C1-C5 alcohols was assessed: MHV1[24] and WS.[25, 26] These two approaches are denoted as PRSV+MHV1+COSMOSAC and PRSV+WS+COSMOSAC and briefly summarized in the following.

The cubic PRSV EOS describes the pressure-volume-temperature relation of a fluid by

$$P = \frac{RT}{v-b} - \frac{a}{v(v+b)+v(v-b)} \quad , \tag{1}$$

where P is the pressure, R the gas constant, T the temperature and v the molar volume. For a pure fluid i, the energy parameter a_i and covolume parameter b_i are determined from the critical temperature $T_{c,i}$, the critical pressure $P_{c,i}$ and the acentric factor ω_i by

$$a_i(T) = 0.457235 \frac{R^2 T_{c,i}^2}{P_{c,i}} \left[1 + \kappa\left(1 - \sqrt{\frac{T}{T_{c,i}}}\right)\right]^2 \quad , \tag{2}$$

$$b_i = 0.077796 \frac{RT_{c,i}}{P_{c,i}} \quad , \tag{3}$$

with

$$\kappa = \kappa_0 + \kappa_{1,i}\left(1 + \sqrt{\frac{T}{T_{c,i}}}\right)\cdot\left(0.7 - \sqrt{\frac{T}{T_{c,i}}}\right) \quad , \tag{4}$$

and

$$\kappa_0 = 0.378893 + 1.4897153\,\omega_i - 0.17131848\,\omega_i^2 + 0.0196654\,\omega_i^3 \, . \tag{5}$$

The species-specific parameter $\kappa_{1,i}$ of pure fluid i was obtained from a regression of experimental vapor pressure data. The employed pure substance parameters were taken from literature and are listed in Table 1. In the case of mixtures, a mixing rule is necessary to determine the temperature and composition dependence of the parameters a and b. Two mixing rules were investigated here: MHV1 and WS.

The energy parameter a and the covolume parameter b are specified by the MHV1 mixing rule by

$$\frac{a}{bRT} = \sum_i^N x_i \left(\frac{a_i}{b_i RT} \right) + \frac{1}{C_{\mathrm{MHV1}}} \left[\frac{G^{ex}}{RT} + \sum_i^N x_i \ln\left(\frac{b}{b_i} \right) \right] \quad , \tag{6}$$

and

$$b = \sum_i^N x_i b_i \quad , \tag{7}$$

where C_{MHV1} = -0.53 is a constant, N the number of components in the mixture, x_i the mole fraction of component i and G^{ex} the excess Gibbs free energy determined from an activity coefficient model, i.e. COSMO-SAC here.

The WS mixing rule defines these two parameters by

$$\frac{a}{b} = \sum_i^N x_i \left(\frac{a_i}{b_i} \right) + \frac{G^{ex}}{C_{\mathrm{WS}}} \quad , \tag{8}$$

and

$$b - \frac{a}{RT} = \sum_i^N \sum_j^N x_i x_j \left(\frac{b_i + b_j}{2} - \frac{\sqrt{a_i a_j}}{RT} \right) \quad , \tag{9}$$

where $C_{\mathrm{WS}} = -\ln(1+\sqrt{2})/\sqrt{2}$ is a constant.

The excess Gibbs free energy needed in eqs 6 and 8 was obtained from the strictly predictive COSMO-SAC model[20] by

$$G^{ex} = RT \sum_i x_i \ln \gamma_i \quad , \tag{10}$$

where the activity coefficient γ_i of component i is determined from the sum of the combinatorial and the residual contributions

$$\ln \gamma_i = \ln \gamma_i^{comb} + \ln \gamma_i^{res} \, . \tag{11}$$

The Staverman−Guggenheim combinatorial term[39, 40] was used to account for molecular size and shape effects

$$\ln \gamma_i^{comb} = 1 - \frac{r_i}{\sum_j x_j r_j} + \ln \frac{r_i}{\sum_j x_j r_j} + \frac{z}{2} q_i \left[\frac{r_i}{q_i} \frac{\sum_j x_j q_j}{\sum_j x_j r_j} + \ln \frac{q_i}{r_i} \frac{\sum_j x_j r_j}{\sum_j x_j q_j} - 1 \right], \quad (12)$$

where z = 10 is the coordination number, while q_i and r_i are the normalized surface area and volume of component i (the standard surface area and volume for normalization were 79.53 Å^2 and 66.69 Å^3). It is worth to mention that the value of standard volume does not influence the calculated results, because it cancels out in eq 12. The residual contribution considers only the electrostatic interactions between unlike components in the mixture. These interactions were determined with COSMO-SAC from the molecular surface screening charge density, which can be obtained from quantum mechanical solvation calculations.[41] In this study, the quantum mechanical results were taken from a free online database from the group of Liu at the Virginia Polytechnic Institute and State University.[42, 43] The σ-profile $p_i(\sigma)$ is a histogram of surface area of segments with the charge density σ on the molecular surface of component i. For mixtures, the σ-profile $p_M(\sigma)$ is determined from

$$p_M(\sigma) = \frac{\sum_i x_i A_i p_i(\sigma)}{\sum_i x_i A_i} \quad . \quad (13)$$

For a better description of the hydrogen bonding interactions, two modifications were introduced into the COSMO-SAC model.[20, 22] First, the σ-profile was separated into three contributions by categorizing the molecular surface into three types: segments of non-hydrogen bonding (nhb) atoms, hydroxyl (OH) groups and other (OT) hydrogen bonding atoms (i.e. O, N, F and H bound to N and F), respectively. The total σ-profile is thus $p_i(\sigma) = p_i^{\text{nhb}}(\sigma) + p_i^{\text{OH}}(\sigma) + p_i^{\text{OT}}(\sigma)$.[20, 44] Second, a Gaussian-type function $f(\sigma) = 1 - \exp(\sigma^2 / 2\sigma_0^2)$ with σ_0 = 0.007 (e·Å^{-2})[22] was used to account for the probability of OH and OT segments to form a hydrogen bond. The segment activity coefficient Γ of a segment with the charge density σ_m in solution j (j is i for

the pure fluid or *M* for the mixture) is determined from

$$\ln \Gamma_j^s(\sigma_m^s) = -\ln\left\{\sum_t^{\text{nhb, OH, OT}} \sum_{\sigma_n} p_j^t(\sigma_n^t)\Gamma_j^t(\sigma_n^t)\exp\left[\frac{-\Delta W(\sigma_m^s, \sigma_n^t)}{RT}\right]\right\}, \quad (14)$$

where the superscripts *s* and *t* represent the property for a segment of type nhb, OH or OT. $\Delta W(\sigma_m^s, \sigma_n^t)$ is the electrostatic interaction between segment *m* (of type *s*) and segment *n* (of type *t*) with the charge densities σ_m^s and σ_n^t

$$\Delta W(\sigma_m^s, \sigma_n^t) = c_{\text{ES}}\left(\sigma_m^s + \sigma_n^t\right)^2 - c_{\text{hb}}(\sigma_m^s, \sigma_n^t)(\sigma_m^s - \sigma_n^t)^2 \ , \quad (15)$$

with the interaction coefficients $c_{\text{ES}}/(\text{kcal}\cdot\text{mol}^{-1}\cdot\text{Å}^4\cdot\text{e}^{-2}) = 6525.69 + 1.4859\cdot10^8/(T/\text{K})^2$ and

$$c_{\text{hb}}(\sigma_m^s, \sigma_n^t)/(\text{kcal}\cdot\text{mol}^{-1}\cdot\text{Å}^4\cdot\text{e}^{-2}) = \begin{cases} 4013.78 & \text{if } s = t = \text{OH and } \sigma_m^s \cdot \sigma_n^t < 0 \\ 932.31 & \text{if } s = t = \text{OT and } \sigma_m^s \cdot \sigma_n^t < 0 \\ 3016.43 & \text{if } s = \text{OH, } t = \text{OT, and } \sigma_m^s \cdot \sigma_n^t < 0 \\ 0 & \text{otherwise.} \end{cases}$$

(16)

The global parameter values of the COSMO-SAC model were taken from the literature without any modification. Details can be found in Ref.[20]

3. Results and discussion

3.1 Experimental results of CO_2 + 2,2-dimethyl-1-propanol

The VLE of the system CO_2 + 2,2-dimethyl-1-propanol was measured at temperatures of 333.2 K and 353.2 K and pressures of up to 12.8 MPa with respect to the saturated liquid line as shown in Figure 3. Numerical VLE data are listed in Table 2. In Figure 3, an almost linear relationship between the mole fraction of CO_2 and the vapor pressure can be identified, if the system is far from the critical line of the mixture. With increasing mole fraction x_{CO2}, this relationship exhibits a logarithmic

shape, i.e. the vapor pressure slowly approaches the critical pressure. This tendency was also observed for all other CO2 + C1-C5 alcohol mixtures around these temperatures.

3.2 Overview on VLE predictions for CO_2 + C1-C5 alcohols

VLE predictions with PRSV+MHV1+COSMOSAC and PRSV+WS+COSMOSAC were investigated for CO_2 + all 16 C1-C5 alcohols. The experimental data considered in this work were retrieved from the Dortmund database,[45] except for CO_2 + 2,2-dimethyl-1-propanol. For some systems, such as CO_2 + methanol or ethanol, experimental data are available for numerous isotherms. Depending on the availability of data for the less popular alcohols, four temperatures were selected in this study: 313.15 K and 333.15 K as well as the highest and lowest temperatures in the database. 313.15 K and 333.15 K were chosen, because most of the CO_2 + alcohol mixtures were measured at around one or both of these temperatures. For most systems, the lowest temperature was below the critical temperature of CO_2, $T_{c,CO2}$ = 304.2 K.

Figure 4 shows a comparison of experimental data and the predictive results from PRSV+MHV1+COSMOSAC and PRSV+WS+COSMOSAC for CO_2 + ethanol at 283.3 K, 313.15 K, 333.15 K and 453.15 K. For the sub-critical isotherm 283.3 K, the VLE envelope was well predicted by PRSV+MHV1+COSMOSAC, while PRSV+WS+COSMOSAC underestimated the vapor pressure. For temperatures somewhat above $T_{c,CO2}$, i.e. at 313.15 K and 333.15 K, PRSV+MHV1+COSMOSAC provides satisfactory results for states that are far away from the critical line of the mixture (or at lower x_{CO2}), but overestimates the vapor pressure if x_{CO2} approaches the critical line of the mixture. On the other hand, PRSV+WS+COSMOSAC always

underestimates the vapor pressure, except for compositions near the critical line. This tendency can also be seen in the phase diagram at the highest temperature 453.15 K.

There are two interesting phenomena that are worth to mention. First, there is an inconsistency between different sets of experimental data. The difference for the vapor pressure at 313.15 K at $x_{CO2} \approx 0.45$ mol·mol^{-1} by Yao et al.[46] and by Qi et al.[47] is about 1.2 MPa. This is significantly larger than the experimental uncertainty that these authors claimed in their publications. Second, PRSV+MHV1+COSMOSAC indicates the existence of a LLE for CO_2 + ethanol at 313.15 K. It can be seen in Figure 4(b) that there is a turning point around $x_{CO2} \approx 0.7$ mol·mol^{-1}. However, a study by Lam et al.[48] has shown experimentally that the system CO_2 + ethanol does not exhibit a LLE.

It has been pointed out in the literature that in order to accurately describe VLE of CO_2 + alcohol mixtures from the combination of the PR EOS and the van der Waals one fluid mixing rule with two adjustable binary interaction parameters (k_{ij} and l_{ij}), experimental data over certain temperature should be chosen as a training set for k_{ij} and l_{ij}.[17, 49] This is an indication that it is a challenging task to adequately predict the fluid phase behavior of CO_2 + alcohol mixtures over a large temperature and composition range.

A comparison of experimental data and the predictive results from PRSV+MHV1+COSMOSAC and PRSV+WS+COSMOSAC for CO_2 + 2-propanol at 293.25 K, 313.15 K, 333.15 K and 443.46 K is shown in Figure 5. At 293.25 K and 313.15 K, the predicted VLE envelope from PRSV+MHV1+COSMOSAC is in good agreement with the experimental data, while PRSV+WS+COSMOSAC again underestimates the vapor pressure. Furthermore, PRSV+MHV1+COSMOSAC does not predict a LLE for this system. At higher temperatures of 333.15 K and 443.46 K, a similar tendency as for the mixture of CO_2 + ethanol at higher temperatures was

found.

Overall, the VLE prediction for CO_2 + C1-C5 alcohols can be categorized into two types according to the prediction from PRSV+MHV1+COSMOSAC: type CO_2 + ethanol or type CO_2 + 2-propanol. Basically, all alcohols considered in this work with the hydroxyl group bound to first carbon atom, such as *n*-alcohols, can be categorized into type CO_2 + ethanol; all others are of type CO_2 + 2-propanol. The results for CO_2 + 1-butanol, as shown in Figure 6, can be considered as another example for type CO_2 + ethanol. However, the only exception is the system CO_2 + 2,2-dimethyl-1-propanol (Figure 3), which has its hydroxyl group bound to the first carbon atom, but with predictive results of type CO_2 + 2-propanol. VLE phase diagrams for all 16 studied CO_2 + C1-C5 alcohol systems can be found in the supporting information. In summary, the VLE prediction for CO_2 + C1-C5 alcohols from PRSV+MHV1+COSMOSAC is clearly superior to that from PRSV+WS+COSMOSAC.

3.3 Capability with respect to similar molecules including isomers

On the basis of quantum mechanical calculations only, the COSMO-SAC model is able to distinguish very similar molecules including isomers.[12, 50] This feature was studied by comparing predicted results for (a) CO_2 + C1-C5 *n*-alcohols, (b) CO_2 + propanols and (c) CO_2 + butanols.

The comparison of experimental data and predicted results for the five mixtures CO_2 + methanol, ethanol, 1-propanol, 1-butanol and 1-pentanol at 313.15 K is shown in Figure 7. The experimental data for these five mixtures, especially for the saturated liquid line, are close to each other. The predictions from PRSV+MHV1+COSMOSAC have a similar tendency as the experimental data before a false LLE is predicted,

except for CO_2 + methanol. PRSV+WS+COSMOSAC shows a very different vapor pressure for the same CO_2 content (especially at around equimolar composition) for different mixtures. This is additional evidence that PRSV+MHV1+COSMOSAC is superior to PRSV+WS+COSMOSAC for CO2 + alcohols. Furthermore, both methods correctly predict the vapor phase composition in the saturated vapor phase for the different mixtures at low pressures.

Figure 8 compares the experimental data and the predicted results of CO_2 + 1-propanol and 2-propanol around 293.2 K and at 313.15 K. The experimental vapor pressure of CO_2 + 1-propanol is higher than that of CO_2 + 2-propanol at the same x_{CO2} for both temperatures. This phenomenon was adequately predicted by both models, but PRSV+WS+COSMOSAC underestimates the vapor pressure throughout the whole composition range. The experimental data and the predicted results for CO_2 + 1-butanol, 2-butanol, 2-methyl-1-propanol and 2-methyl-2-propanol at 313.15 K are compared in Figure 9. As can be seen, the experiments yield a sequence for the vapor pressure at $x_{CO2} \approx 0.5$ mol·mol^{-1} (from highest to lowest): CO_2 + 1-butanol, 2-methyl-1-propanol, 2-butanol and 2-methyl-2-propanol. Both approaches accurately predict this sequence, but none is able to yield the experimentally observed high mole fraction of 2-methyl-1-propanol in the saturated vapor phase at low pressures.

3.4 Case study for drug solubility prediction

The drug solubility is important for process optimization in the pharmaceutical industry. The COSMO-SAC model is a complementary method to estimate the solubility of solid drugs in organic solvents under ambient conditions when no experimental drug solubility data are available.[12, 13, 51] In this section, a case study for the solubility of the two anti-inflammatory drugs naproxen and ibuprofen in CO_2 +

ethanol mixtures at 298 K and 10 MPa is conducted to investigate the applicability of the present approaches. The critical temperature, the critical pressure and the acentric factor are pure substance properties, that are necessary for cubic EOS. In addition, the normal melting temperature and the heat of fusion are necessary for the drug solubility calculation. These pure substance parameters for naproxen and ibuprofen are summarized in Table 3.

The comparison of experimental data and the predictive results from PRSV+MHV1+COSMOSAC and PRSV+WS+COSMOSAC for the solubility of naproxen and ibuprofen in CO_2 + ethanol mixtures at 298 K and 10 MPa are shown in Figure 10. Both drugs have a high solubility in pure ethanol and a very low solubility in pure CO_2 and their solubility decreases with increasing mole fraction of CO_2 in the mixture solvents. PRSV+MHV1+COSMOSAC describes this tendency correctly and the deviations from experimental data are within one log-unit throughout the entire composition range. PRSV+WS+COSMOSAC provides a good prediction for the solubility of both drugs in pure ethanol, but overestimates it in pure CO_2. Therefore, PRSV+WS+COSMOSAC exhibits larger deviations for higher CO_2 content and predicts a maximum solubility of naproxen in CO_2 + ethanol mixtures. This case study shows that these two approaches can be applied to estimate the solubility of other drugs in this type of mixtures, because there is no issue of missing parameters.

5. Conclusions

Experimental VLE data for the binary mixture of CO_2 + 2,2-dimethyl-1-propanol were measured with a high pressure view cell technique based on the synthetic method at 313.2 K and 333.2 K in the pressure range from 5.33 to 12.8 MPa. With these new data, experimental VLE data are now available for all binary mixtures of

CO_2 + C1-C5 alcohols. The predictive power of fully predictive models for these 16 binary mixtures was investigated, i.e. the combination of the PRSV EOS with the COSMO-SAC model through the MHV1 mixing rule or alternatively the WS mixing rule without any binary interaction parameters. The predicted results were compared with the available literature data for all CO_2 + C1-C5 alcohols at four selected temperatures from sub-critical to supercritical CO_2 conditions, depending on the availability of experimental data. PRSV+MHV1+COSMOSAC provides satisfactory VLE predictions for these 16 binary mixtures if the systems are far from the critical line of the mixture, while PRSV+WS+COSMOSAC provides better predictions when the systems are near the critical line. Although both models only provide qualitatively correct predictions, they could be viable methods for estimating the solubility of new drugs in this type of mixtures, because there is no issue of missing parameters for these models.

Acknowledgements

The authors would like to thank the financial support from the Alexander von Humboldt Stiftung. We wish to thank Prof. Shiang-Tai Lin and Li-Hsin Wang at National Taiwan University for valuable discussions and Elmar Baumhögger for his support in the experimental investigations.

Supporting Information Available: Detailed results for all binary systems considered in this work. This information is available free of charge via the Internet at http://pubs.acs.org.

Reference:

(1) Cooper, A. I., Polymer synthesis and processing using supercritical carbon dioxide. *J. Mater. Chem.* **2000,** 10, 207-234.

(2) Brunner, G., Supercritical fluids: technology and application to food processing. *J. Food Eng.* **2005,** 67, 21-33.

(3) Araus, K. A.; Canales, R. I.; del Valle, J. M.; de la Fuente, J. C., Solubility of beta-carotene in ethanol- and triolein-modified CO2. *J. Chem. Thermodyn.* **2011,** 43, 1991-2001.

(4) De Zordi, N.; Kikic, I.; Moneghini, M.; Solinas, D., Solubility of pharmaceutical compounds in supercritical carbon dioxide. *J. Supercrit. Fluids* **2012,** 66, 16-22.

(5) Temelli, F.; Cordoba, A.; Elizondo, E.; Cano-Sarabia, M.; Veciana, J.; Ventosa, N., Phase behavior of phytosterols and cholesterol in carbon dioxide-expanded ethanol. *J. Supercrit. Fluids* **2012,** 63, 59-68.

(6) Girotra, P.; Singh, S. K.; Nagpal, K., Supercritical fluid technology: a promising approach in pharmaceutical research. *Pharm. Dev. Technol.* **2013,** 18, 22-38.

(7) Merker, T.; Hsieh, C. M.; Lin, S. T.; Hasse, H.; Vrabec, J., Fluid-phase coexistence for the oxidation of CO2 expanded cyclohexane: Experiment, molecular simulation, and COSMO-SAC. *AIChE J.* **2013,** 59, 2236-2250.

(8) Ciftci, O. N.; Calderon, J.; Temelli, F., Supercritical carbon dioxide extraction of corn distiller's dried grains with solubles: Experiments and mathematical modeling. *J. Agric. Food Chem.* **2012,** 60, 12482-12490.

(9) Camy, S.; Condoret, J. S., Modelling and experimental study of separators for co-solvent recovery in a supercritical extraction process. *J. Supercrit. Fluids* **2006,** 38, 51-61.

(10) Sandler, S. I., *Chemical and Engineering Thermodynamics*. 3rd ed.; John Wiley & Sons: New York, 1999.

(11) Poling, B. E.; Prausnitz, J. M.; O'Connell, J. P., *The Properties of Gases and Liquids* 5th ed.; McGraw-Hill: New York, 2001.

(12) Hsieh, C.-M.; Wang, S.; Lin, S.-T.; Sandler, S. I., A predictive model for the solubility and octanol-water partition coefficient of pharmaceuticals. *J. Chem. Eng. Data* **2011,** 56, 936-945.

(13) Tung, H.-H.; Tabora, J.; Variankaval, N.; Bakken, D.; Chen, C.-C., Prediction of pharmaceutical solubility via NRTL-SAC and COSMO-SAC. *J. Pharm. Sci.* **2008,** 97, 1813-1820.

(14) Secuianu, C.; Qian, J. W.; Privat, R.; Jaubert, J. N., Fluid Phase Equilibria Correlation for Carbon Dioxide+1-Heptanol System with Cubic Equations of State. *Ind. Eng. Chem. Res.* **2012,** 51, 11284-11293.

(15) Secuianu, C.; Feroiu, V.; Geana, D., Measurements and modeling of high-pressure phase behavior of the carbon dioxide + pentan-1-ol binary system. *J. Chem. Eng. Data* **2011,** 56, 5000-5007.

(16) Valderrama, J. O.; Zavaleta, J., Generalized binary interaction parameters in the Wong-Sandler mixing rules for mixtures containing n-alkanols and carbon dioxide. *Fluid Phase Equilib.* **2005,** 234, 136-143.

(17) Polishuk, I.; Wisniak, J.; Segura, H., Simultaneous prediction of the critical and sub-critical phase behavior in mixtures using equation of state I. Carbon dioxide-alkanols. *Chem. Eng. Sci.* **2001,** 56, 6485-6510.

(18) Klamt, A., Conductor-like screening model for real solvents - A new approach to the quantitative calculation of solvation phenomena. *J. Phys. Chem.* **1995,** 99, 2224-2235.

(19) Klamt, A.; Jonas, V.; Burger, T.; Lohrenz, J. C. W., Refinement and parametrization of COSMO-RS. *J. Phys. Chem. A* **1998,** 102, 5074-5085.
(20) Hsieh, C. M.; Sandler, S. I.; Lin, S. T., Improvements of COSMO-SAC for vapor-liquid and liquid-liquid equilibrium predictions. *Fluid Phase Equilib.* **2010,** 297, 90-97.
(21) Lin, S.-T.; Sandler, S. I., A priori phase equilibrium prediction from a segment contribution solvation model. *Ind. Eng. Chem. Res.* **2002,** 41, 899-913.
(22) Wang, S.; Sandler, S. I.; Chen, C.-C., Refinement of COSMO-SAC and the applications. *Ind. Eng. Chem. Res.* **2007,** 46, 7275-7288.
(23) Stryjek, R.; Vera, J. H., PRSV - An improved Peng-Robinson equation of state for pure compounds and mixtures. *Can. J. Chem. Eng.* **1986,** 64, 323-333.
(24) Michelsen, M. L., A modified Huron-Vidal mixing rule for cubic equations of state. *Fluid Phase Equilib.* **1990,** 60, 213-219.
(25) Wong, D. S.-H.; Orbey, H.; Sandler, S. I., Equation of state mixing rule for nonideal mixtures using available activity-coefficient model parameters and that allows extrapolation over large ranges of temperature and pressure. *Ind. Eng. Chem. Res.* **1992,** 31, 2033-2039.
(26) Wong, D. S.-H.; Sandler, S. I., A theoretically correct mixing rule for cubic equations of state. *AIChE J.* **1992,** 38, 671-680.
(27) Hsieh, M.-K.; Lin, S.-T., Effect of mixing rule boundary conditions on high pressure (liquid + liquid) equilibrium prediction. *J. Chem. Thermodyn.* **2012,** 47, 33-41.
(28) Alvarez, V. H.; Mattedi, S.; Aznar, M., Density, refraction index, and vapor-liquid equilibria of n-methyl-2-hydroxyethylammonium hexanoate plus (methyl acetate, ethyl acetate, or propyl acetate) at several temperatures. *Ind. Eng. Chem. Res.* **2012,** 51, 14543-14554.
(29) Tai, Y.-S.; Hsieh, M.-T.; Lee, M.-T.; Wong, D. S.-H.; Lin, S.-T., A priori predictions of critical loci from the combined use of PRSV equation of state and the COSMO-SAC model through the MHV1 mixing rule. *Fluid Phase Equilib.* **2011,** 308, 25-34.
(30) Leonhard, K.; Veverka, J.; Lucas, K., A Comparison of mixing rules for the combination of COSMO-RS and the Peng-Robinson equation of state. *Fluid Phase Equilib.* **2009,** 275, 105-115.
(31) Lee, M.-T.; Lin, S.-T., Prediction of mixture vapor-liquid equilibrium from the combined use of Peng-Robinson equation of state and COSMO-SAC activity coefficient model through the Wong-Sandler mixing rule. *Fluid Phase Equilib.* **2007,** 254, 28-34.
(32) Hsieh, C.-M.; Lin, S.-T., First-principles predictions of vapor-liquid equilibria for pure and mixture fluids from the combined use of cubic equations of state and solvation calculations. *Ind. Eng. Chem. Res.* **2009,** 48, 3197-3205.
(33) Hsieh, C.-M.; Lin, S.-T., Prediction of 1-octanol-water partition coefficient and infinite dilution activity coefficient in water from the PR plus COSMOSAC model. *Fluid Phase Equilib.* **2009,** 285, 8-14.
(34) Shimoyama, Y.; Abeta, T.; Iwai, Y., Prediction of vapor-liquid equilibria for supercritical alcohol plus fatty acid ester systems by SRK equation of state with Wong-Sandler mixing rule based on COSMO theory. *J. Supercrit. Fluids* **2008,** 46, 4-9.
(35) Windmann, T.; Koster, A.; Vrabec, J., Vapor-liquid equilibrium measurements of the binary mixtures nitrogen + acetone and oxygen + acetone. *J. Chem. Eng. Data* **2012,** 57, 1672-1677.

(36) Span, R.; Wagner, W., A new equation of state for carbon dioxide covering the fluid region from the triple-point temperature to 1100 K at pressures up to 800 MPa. *J. Phys. Chem. Ref. Data* **1996,** 25, 1509-1596.
(37) Myers, R. S.; Clever, H. L., Surface tension and density of some hydrocarbon + alcohol mixtures at 303.15 K. *J. Chem. Thermodyn.* **1974,** 6, 949-955.
(38) Costello, J. M.; Bowden, S. T., The temperature variation of orthobaric density difference in liquid-vapour system .3. Alcohols. *Recl. Trav. Chim. Pays-Bas-J. Roy. Neth. Chem. Soc.* **1958,** 77, 36-46.
(39) Staverman, A. J., The entropy of high polymer solutions - Generalization of formulae. *Recl. Trav. Chim. Pays-Bas-J. Roy. Neth. Chem. Soc.* **1950,** 69, 163-174.
(40) Guggenheim, E. A., *Mixtures*. Oxford University Press: Oxford, 1952.
(41) Klamt, A.; Schuurmann, G., COSMO - A new approach to dielectric screening in solvents with explicit expressions for the screening energy and its gradient. *J. Chem. Soc.-Perkin Trans. 2* **1993**, 799-805.
(42)Mullins, E.; Oldland, R.; Liu, Y. A.; Wang, S.; Sandler, S. I.; Chen, C.-C.; Zwolak, M.; Seavey, K. C., Sigma-profile database for using COSMO-based thermodynamic methods. *Ind. Eng. Chem. Res.* **2006,** 45, 4389-4415.
(43) Stoll, J.; Vrabec, J.; Hasse, H.; Fischer, J., Comprehensive study of the vapour-liquid equilibria of the pure two-centre Lennard-Jones plus pointquadrupole fluid. *Fluid Phase Equilib.* **2001,** 179, 339-362.
(44) Hsieh, C.-M.; Lin, S.-T., Prediction of liquid-liquid equilibrium from the Peng-Robinson plus COSMOSAC equation of state. *Chem. Eng. Sci.* **2010,** 65, 1955-1963.
(45) Mu, T.; Rarey, J.; Gmehling, J., Performance of COSMO-RS with sigma profiles from different model chemistries. *Ind. Eng. Chem. Res.* **2007,** 46, 6612-6629.
(46) Yao, S.; Liu, F.; Han, Z.; Zhu, Z., Vapor-liquid equilibria of binary systems of alcohols, water-carbon dioxide at supercritical or near critical condition. *J. Chem. Eng. Chinese U.* **1989,** 3, 9-15.
(47) Qi, G.; Fu, J.; Sun, X.; Zhao, S., Gas-liquid equilibrium data of CO2-chloroaluminate ionic liquid benzene ternary system. *Petrochem. Technol.* **2008,** 37, 262-266.
(48) Lam, D. H.; Jangkamolkulchai, A.; Luks, K. D., Liquid-liquid-vapor phase equilibrium behavior of centain binary carbon dioxide + n-alkanol mixtures. *Fluid Phase Equilib.* **1990,** 60, 131-141.
(49) Secuianu, C.; Feroiu, V.; Geană, D., Phase behavior for carbon dioxide + ethanol system: Experimental measurements and modeling with a cubic equation of state. *J. Supercrit. Fluids* **2008,** 47, 109-116.
(50) Hsieh, C.-M.; Lin, S.-T., First-principles prediction of phase equilibria using the PR+COSMOSAC equation of state. *Asia-Pac. J. Chem. Eng.* **2012,** 7, S1-S10.
(51) Shu, C. C.; Lin, S. T., Prediction of drug solubility in mixed solvent systems using the COSMO-SAC activity coefficient model. *Ind. Eng. Chem. Res.* **2011,** 50, 142-147.
(52) Mathews, J. F., Critical constants of inorganic substances. *Chem. Rev.* **1972,** 72, 71-100.
(53) Orbey, H.; Sandler, S. I., *Modeling Vapor-Liquid Equilibria: Cubic Equations of State and Their Mixing Rules.* Cambridge University Press: New York, 1998.
(54) Ambrose, D.; Walton, J., Vapor-pressures up to their critical-temperatures of normal alkanes and 1-alkanols. *Pure Appl. Chem.* **1989,** 61, 1395-1403.
(55) Gude, M.; Teja, A. S., Vapor-liquid critical properties of elements and

compounds .4. Aliphatic alkanols. *J. Chem. Eng. Data* **1995,** 40, 1025-1036.
(56) Teja, A. S.; Lee, R. J.; Rosenthal, D.; Anselme, M., Correlation of the critical properties of alkanes and alkanols. *Fluid Phase Equilib.* **1990,** 56, 153-169.
(57) Hernandez, P.; Ortega, J., Vapor-liquid equilibria and densities for ethyl esters (ethanoate to butanoate) and alkan-2-ol (C-3-C-4) at 101.32 kPa. *J. Chem. Eng. Data* **1997,** 42, 1090-1100.
(58) Riddick, J. A.; Bunger, W. B.; Sakano, T. K., *Organic Solvents: Physical Properties and Methods of Purification*. 4th ed.; Wiley Interscience: New York, 1986.
(59) Ambrose, D., *Vapor-Liquid Critical Properties*. Middlesex: United Kingdom, 1980.
(60) Kudchadk, A. P.; Alani, G. H.; Zwolinski, B. J., Critical constants of organic substances. *Chem. Rev.* **1968,** 68, 659-735.
(61) Lee, H. S.; Mun, S. Y.; Lee, H., High-pressure phase equilibria for the carbon dioxide + 3-pentanol and carbon dioxide + 3-pentanol + water systems. *J. Chem. Eng. Data* **1999,** 44, 524-527.
(62) Daubert, T. E.; Danner, R. P., *Technical Data Book - Petroleum Refining* 6th ed.; American Petroleum Institute: Washington D.C., 1997.
(63) Marrero-Morejon, J.; Pardillo-Fontdevila, E., Estimation of pure compound properties using group-interaction contributions. *Aiche J.* **1999,** 45, 615-621.
(64) Bozbag, S. E.; Erkey, C., Supercritical fluids in fuel cell research and development. *J. Supercrit. Fluids* **2012,** 62, 1-31.
(65) Coimbra, P.; Duarte, C. M. M.; de Sousa, H. C., Cubic equation-of-state correlation of the solubility of some anti-inflammatory drugs in supercritical carbon dioxide. *Fluid Phase Equilib.* **2006,** 239, 188-199.
(66) Neau, S. H.; Bhandarkar, S. V.; Hellmuth, E. W., Differential molar heat capacities to test ideal solubility estimations. *Pharm. Res.* **1997,** 14, 601-605.
(67) Lyderden, A. L., *Estimation of Critical Properties of Organic Compounds*. University of Wisconsin College Engineering: Madison, Wisconsin, 1995.
(68) Private Communication, J. David Chase, Hoechst Celanese (January 9, 1995).
(69) Elkordy, A. A.; Essa, E. A., Dissolution of ibuprofen from spray dried and spray chilled particles. *Pak. J. Pharm. Sci.* **2010,** 23, 284-290.
(70) Hirohama, S.; Takatsuka, T.; Miyamoto, S.; Muto, T., Measument and correlation of phase equilibria for the carbon dioxide-ethanol-water system. *J. Chem. Eng. Jpn.* **1993,** 26, 408-415.
(71) Galicia-Luna, L. A.; Ortega-Rodriguez, A.; Richon, D., New apparatus for the fast determination of high-pressure vapor−liquid equilibria of mixtures and of accurate critical pressures. *J. Chem. Eng. Data* **2000,** 45, 265-271.
(72) Stievano, M.; Elvassore, N., High-pressure density and vapor–liquid equilibrium for the binary systems carbon dioxide–ethanol, carbon dioxide–acetone and carbon dioxide–dichloromethane. *J. Supercrit. Fluids* **2005,** 33, 7-14.
(73) Kato, M.; Kodama, D.; Ono, T.; Kokubo, M., Volumetric properties of carbon dioxide + ethanol at 313.15 K. *J. Chem. Eng. Data* **2009,** 54, 2953-2956.
(74) Tian, Y. L.; Han, M.; Chen, L.; Feng, J. J.; Qin, Y., Study on vapor-liquid phase equilibria for CO2-C2H5OH system. *Acta Phys.-Chim. Sin.* **2001,** 17, 155-160.
(75) Zhu, H. G.; Tian, Y. L.; Chen, L.; Feng, J. J.; Fu, H. F., Studies on vapor-liquid phase equilibria for SCF CO2+CH3OH and SCF CO2+C2H5OH systems. *Chem. J. Chin. Univ.-Chin.* **2002,** 23, 1588-1591.
(76) Elizalde-Solis, O.; Galicia-Luna, L. A., Solubility of thiophene in carbon dioxide and carbon dioxide + 1-propanol mixtures at temperatures from 313 to 363 K.

Fluid Phase Equilib. **2005,** 230, 51-57.
(77) Secuianu, C.; Feroiu, V.; Geană, D., High-pressure vapor−liquid equilibria in the system carbon dioxide and 2-propanol at temperatures from 293.25 K to 323.15 K. *J. Chem. Eng. Data* **2003,** 48, 1384-1386.
(78) Yaginuma, R.; Nakajima, T.; Tanaka, H.; Kato, M., Densities of carbon dioxide + 2-propanol at 313.15 K and pressures to 9.8 MPa. *J. Chem. Eng. Data* **1997,** 42, 814-816.
(79) Lim, J. S.; Jung, Y. G.; Yoo, K.-P., High-pressure vapor−liquid equilibria for the binary mixtures of carbon dioxide + isopropanol (IPA). *J. Chem. Eng. Data* **2007,** 52, 2405-2408.
(80) Elizalde-Solis, O.; Galicia-Luna, L. A.; Camacho-Camacho, L. E., High-pressure vapor–liquid equilibria for CO2 + alkanol systems and densities of n-dodecane and n-tridecane. *Fluid Phase Equilib.* **2007,** 259, 23-32.
(81) Secuianu, C.; Feroiu, V.; Geană, D., High-pressure vapor−liquid equilibria in the system carbon dioxide + 1-butanol at temperatures from (293.15 to 324.15) K. *J. Chem. Eng. Data* **2004,** 49, 1635-1638.
(82) Ishihara, K.; Tsukajima, A.; Tanaka, H.; Kato, M.; Sako, T.; Sato, M.; Hakuta, T., Vapor−liquid equilibrium for carbon dioxide + 1-butanol at high pressure. *J. Chem. Eng. Data* **1996,** 41, 324-325.
(83) Lim, J.-S.; Yoon, C.-H.; Yoo, K.-P., High-pressure vapor-liquid equilibrium measurement for the binary mixtures of carbon dioxide + n-butanol. *Korean J. Chem. Eng.* **2009,** 26, 1754-1758.
(84) Chen, H.-I.; Chang, H.-Y.; Chen, P.-H., High-pressure phase equilibria of carbon dioxide + 1-butanol, and carbon dioxide + water + 1-butanol systems. *J. Chem. Eng. Data* **2002,** 47, 776-780.
(85) Joung, S. N.; Yoo, C. W.; Shin, H. Y.; Kim, S. Y.; Yoo, K.-P.; Lee, C. S.; Huh, W. S., Measurements and correlation of high-pressure VLE of binary CO2–alcohol systems (methanol, ethanol, 2-methoxyethanol and 2-ethoxyethanol). *Fluid Phase Equilib.* **2001,** 185, 219-230.
(86) Kodama, D.; Kubota, N.; Yamaki, Y.; Tanaka, H.; Kato, M., High pressure vapor-liquid equilibria and density behaviors for carbon dioxide + methanol system at 313.15K. *Netsu Bussei* **1996,** 10, 16-20.
(87) Laursen, T.; Rasmussen, P.; Andersen, S. I., VLE and VLLE measurements of dimethyl ether containing systems. *J. Chem. Eng. Data* **2002,** 47, 198-202.
(88) Ohgaki, K.; Katayama, T., Isothermal vapor-liquid equilibrium data for binary systems containing carbon dioxide at high pressures: methanol-carbon dioxide, n-hexane-carbon dioxide, and benzene-carbon dioxide systems. *J. Chem. Eng. Data* **1976,** 21, 53-55.
(89) Naidoo, P.; Ramjugernath, D.; Raal, J. D., A new high-pressure vapour-liquid equilibrium apparatus. *Fluid Phase Equilib.* **2008,** 269, 104-112.
(90) Secuianu, C.; Feroiu, V.; Geană, D., High-pressure phase equilibria for the carbon dioxide + 1-propanol system. *J. Chem. Eng. Data* **2008,** 53, 2444-2448.
(91) Yim, J.-H.; Jung, Y. G.; Lim, J. S., Vapor-liquid equilibria of carbon dioxide+n-propanol at elevated pressure. *Korean J. Chem. Eng.* **2010,** 27, 284-288.
(92) Silva-Oliver, G.; Galicia-Luna, L. A.; Sandler, S. I., Vapor–liquid equilibria and critical points for the carbon dioxide +1-pentanol and carbon dioxide +2-pentanol systems at temperatures from 332 to 432 K. *Fluid Phase Equilib.* **2002,** 200, 161-172.
(93) Secuianu, C.; Feroiu, V.; Geană, D., Phase behavior for the carbon dioxide +

2-butanol system: Experimental measurements and modeling with cubic equations of state. *J. Chem. Eng. Data* **2009,** 54, 1493-1499.
(94) da Silva, M. V.; Barbosa, D., High pressure vapor–liquid equilibrium data for the systems carbon dioxide/2-methyl-1-propanol and carbon dioxide/3-methyl-1-butanol at 288.2, 303.2 and 313.2 K. *Fluid Phase Equilib.* **2002,** 198, 229-237.
(95) Stradi, B. A.; Kohn, J. P.; Stadtherr, M. A.; Brennecke, J. F., Phase behavior of the reactants, products and catalysts involved in the allylic epoxidation of trans-2-Hexen-1-ol to (2R,3R)-(+)-3-Propyloxiranemethanol in high pressure carbon dioxide. *J. Supercrit. Fluids* **1998,** 12, 109-122.
(96) Heo, J.-H.; Shin, H. Y.; Park, J.-U.; Joung, S. N.; Kim, S. Y.; Yoo, K.-P., Vapor−liquid equilibria for binary mixtures of CO2 with 2-methyl-2-propanol, 2-methyl-2-butanol, octanoic acid, and decanoic acid at temperatures from 313.15 K to 353.15 K and pressures from 3 MPa to 24 MPa. *J. Chem. Eng. Data* **2001,** 46, 355-358.
(97) Munto, M.; Ventosa, N.; Sala, S.; Veciana, J., Solubility behaviors of ibuprofen and naproxen drugs in liquid "CO2-organic solvent" mixtures. *J. Supercrit. Fluids* **2008,** 47, 147-153.

Tables

Table 1. Pure substance parameters of the PRSV EOS

Compound	T_c/K	P_c/MPa	ω [a]	κ_1 [a]
carbon dixoide	304.2 [52]	7.382 [53]	0.225 [53]	0
methanol	512.64 [54]	8.092 [54]	0.564 [54]	-0.159565
Ethanol	514 [55]	6.137 [55]	0.643 [54]	-0.052957
1-propanol	536.78 [54]	5.168 [54]	0.62 [54]	0.159438
2-propanol	508.3 [56]	4.762 [56]	0.668 [57]	0.155693
1-butanol	563.05 [54]	4.424 [54]	0.591 [54]	0.293169
2-butanol	536.05 [58]	4.194 [58]	0.577 [59]	0.376143
2-methyl-1-propanol	547.78 [59]	4.295 [60]	0.592 [59]	0.379802
2-methyl-2-propanol	506.2 [60]	3.972 [60]	0.612 [60]	0.40761
1-pentanol	588.15 [54]	3.909 [54]	0.579 [54]	0.278242
2-pentanol	560.3 [55]	3.675 [55]	0.555	0.476929
3-pentanol	559.6 [55]	3.99 [61]	0.547 [61]	0.367144
2-methyl-1-butanol	575.4 [55]	3.94 [55]	0.588	0.314204
2-methyl-2-butanol	543.7 [55]	3.71 [55]	0.4795 [62]	0.510698
3-methyl-1-butanol	579.4 [60]	3.93 [55]	0.59	0.29606
3-methyl-2-butanol	556.1 [55]	3.87 [55]	0.502	0.467261
2,2-dimethyl-1-propanol	552.7 [63]	4.078 [63]	0.595	0.238164

a. κ_1 and ω are estimated by using experimental vapor pressure data from the DIPPR database[64] when they are not available in literature.

Table 2. Experimental vapor−liquid equilibrium data along the saturated liquid line of the mixture CO_2 + 2,2-dimethyl-1-propanol[a] generated in this work

T/K	P/MPa	x_{CO2}/mol·mol^{-1}
333.2	5.09	0.280 (2)
333.2	5.08	0.288 (2)
333.2	6.63	0.405 (2)
333.2	8.07	0.515 (3)
333.2	9.04	0.629 (3)
333.2	10.17	0.788 (4)
333.2	10.66	0.853 (5)
333.2	10.54	0.861 (5)
353.2	5.33	0.267 (1)
353.2	5.87	0.292 (2)
353.2	7.33	0.366 (2)
353.2	9.43	0.492 (3)
353.2	11.07	0.607 (3)
353.2	12.42	0.764 (4)
353.2	12.79	0.837 (5)
353.2	12.80	0.840 (5)

a. $u(T)$ = 0.04 K, $u(P)$ = 0.01 MPa and the numbers in parentheses are $u(x)$ in the last digits.

Table 3. Pure substance parameters of naproxen and ibuprofen

Compound	T_c/K	P_c/MPa	ω	T_m/K	ΔH_{fus}/ J·mol^{-1}
naproxen	807 [65]	2.42 [65]	0.904 [65]	349.48 [66]	26342 [66]
ibuprofen	777 [67]	2.98 [68]	1.01 [a]	428.5 [69]	31500 [69]

a. ω is estimated by using experimental vapor pressure data from the DIPPR database[64]

Figure Caption

Figure 1. Molecular structure of the 16 considered C1-C5 alcohols.

Figure 2. Schematic of the experimental setup for the measurement of the vapor pressure and the saturated liquid composition of CO_2 + 2,2-dimethyl-1-propanol. V1 indicates a valve, TW-V1 a three-way valve, TX a thermometer and PX a pressure transducer.

Figure 3. Comparison of vapor-liquid equilibria of CO_2 + 2,2-dimethyl-1-propanol at 313.2 K (a) and 333.2 K (b) from experiment, this work □ and predictions by PRSV+WS+COSMOSAC --- and PRSV+MHV1+COSMOSAC ─.

Figure 4. Comparison of vapor-liquid equilibria of CO_2 + ethanol at 283.3 K (a), 313.15 K (b), 333.15 K (c) and 453.15 K (d) from experiment and predictions by PRSV+WS+COSMOSAC --- and PRSV+MHV1+COSMOSAC ─. Experimental data were taken from the literature (283.15 K: □ [70]; 313.15 K: □ [46], ◊ [71], Δ [72], ○ [47], **x** [73], **+** [49]; 333.15 K: □ [74], ◊ [75], Δ [76], ○ [49]; 453.15 K: □ [74]).

Figure 5. Comparison of vapor-liquid equilibria of CO_2 + 2-propanol at 293.25 K (a), 313.15 K (b), 333.15 K (c) and 443.46 K (d) from experiment and predictions by PRSV+WS+COSMOSAC --- and PRSV+MHV1+COSMOSAC ─. Experimental data were taken from the literature (293.25 K: □ [77]; 313.15 K: □ [78], ◊ [45]; 333.15 K: □ [45], ◊ [79]; 443.46 K: □ [80]).

Figure 6. Comparison of vapor-liquid equilibria of CO_2 + 1-butanol at 293.15 K (a),

313.15 K (b), 333.15 K (c) and 430.25 K (d) from experiment and predictions by PRSV+WS+COSMOSAC --- and PRSV+MHV1+COSMOSAC ─. Experimental data were taken from the literature (293.15 K: □ [81]; 313.15 K: □ [82], ◊ [45], Δ [81], ○ [83]; 333.15 K: □ [84], ◊ [83]; 430.15 K: □ [80]).

Figure 7. Comparison of vapor-liquid equilibria of CO_2 + C1-C5 *n*-alcohols at 313.15 K from experiment and predictions by PRSV+MHV1+COSMOSAC (a) and PRSV+WS+COSMOSAC (b). The blue lines and diamonds represent experimental and predicted data of CO_2 + methanol,[85-89] respectively; the green lines and circles CO_2 + ethanol;[46, 47, 49, 71-73] the red lines and triangles CO_2 + 1-propanol;[45, 46, 90, 91] the purple lines and crosses CO_2 + 1-butanol;[45, 81-83] the black lines and squares CO_2 + 1-pentanol.[92]

Figure 8. Comparison of vapor-liquid equilibria of CO_2 + propanols around 293.2 K (a) and at 313.15 K (b) from experiment and predictions by PRSV+WS+COSMOSAC --- and PRSV+MHV1+COSMOSAC ─. The black lines and squares represent experimental and predicted results of CO_2 + 1-propanol,[45, 46, 90, 91] respectively; the gray lines and circles CO_2 + 2-propanol.[45, 77, 78]

Figure 9. Comparison of vapor-liquid equilibria of CO_2 + butanols at 313.15 K from experiment and predictions by PRSV+MHV1+COSMOSAC (a) and PRSV+WS+COSMOSAC (b). The blue lines and diamonds represent experimental and predicted data of CO_2 + 1-butanol,[45, 81-83] respectively; the green lines and circles CO_2 + 2-butanol;[93] the red lines and triangles CO_2 + 2-methyl-1-propanol;[45, 94] the black lines and squares CO_2 + 2-methyl-2-propanol.[95, 96]

Figure 10. Comparison of the solubility of naproxen (a) and ibuprofen (b) in CO_2 + ethanol mixtures at 298 K and 10 MPa from experiment □ [97] and predictions by PRSV+MHV1+COSMOSAC ─ and PRSV+WS+COSMOSAC ---.

Figures

Figure 1.

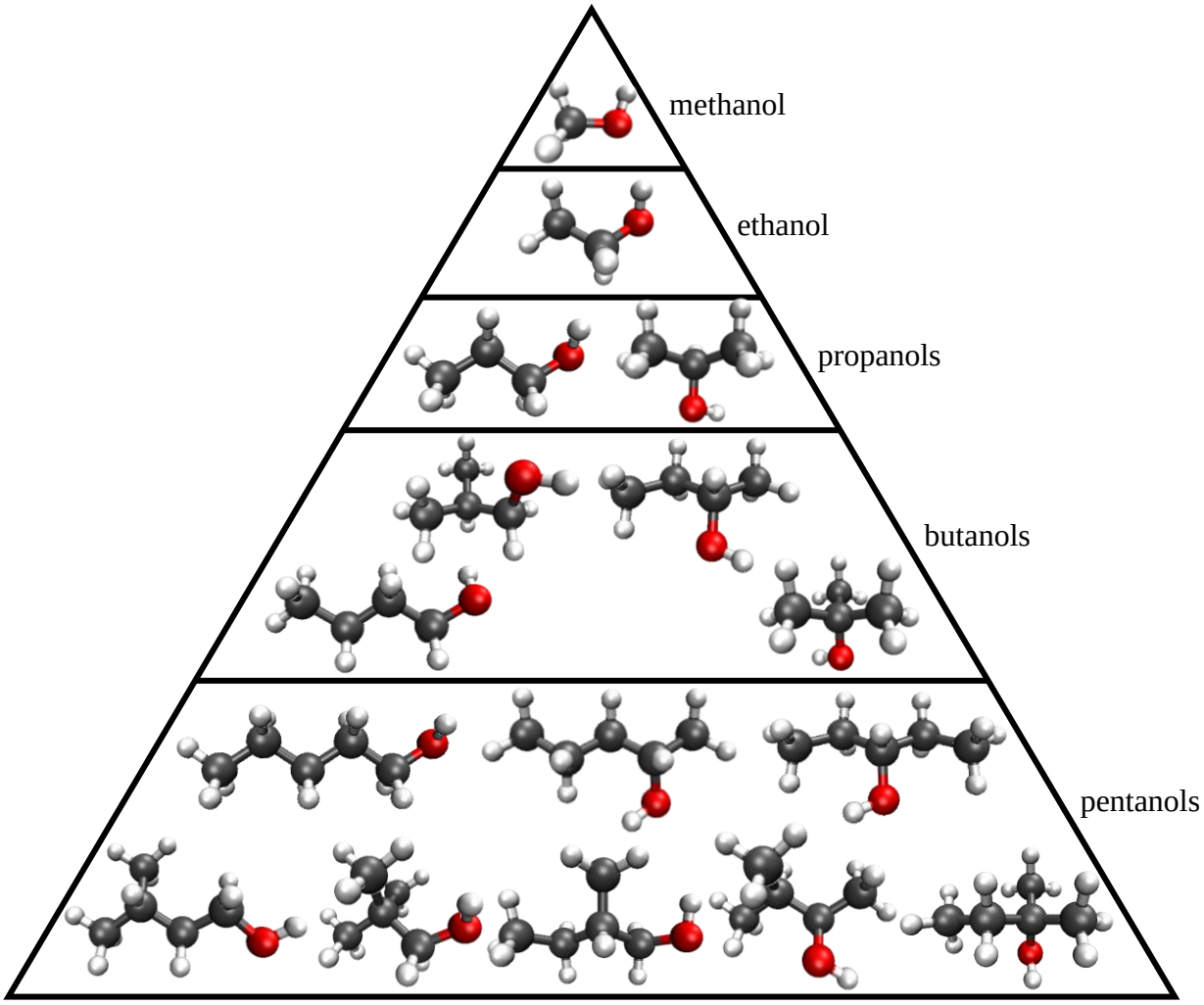

Figure 2.

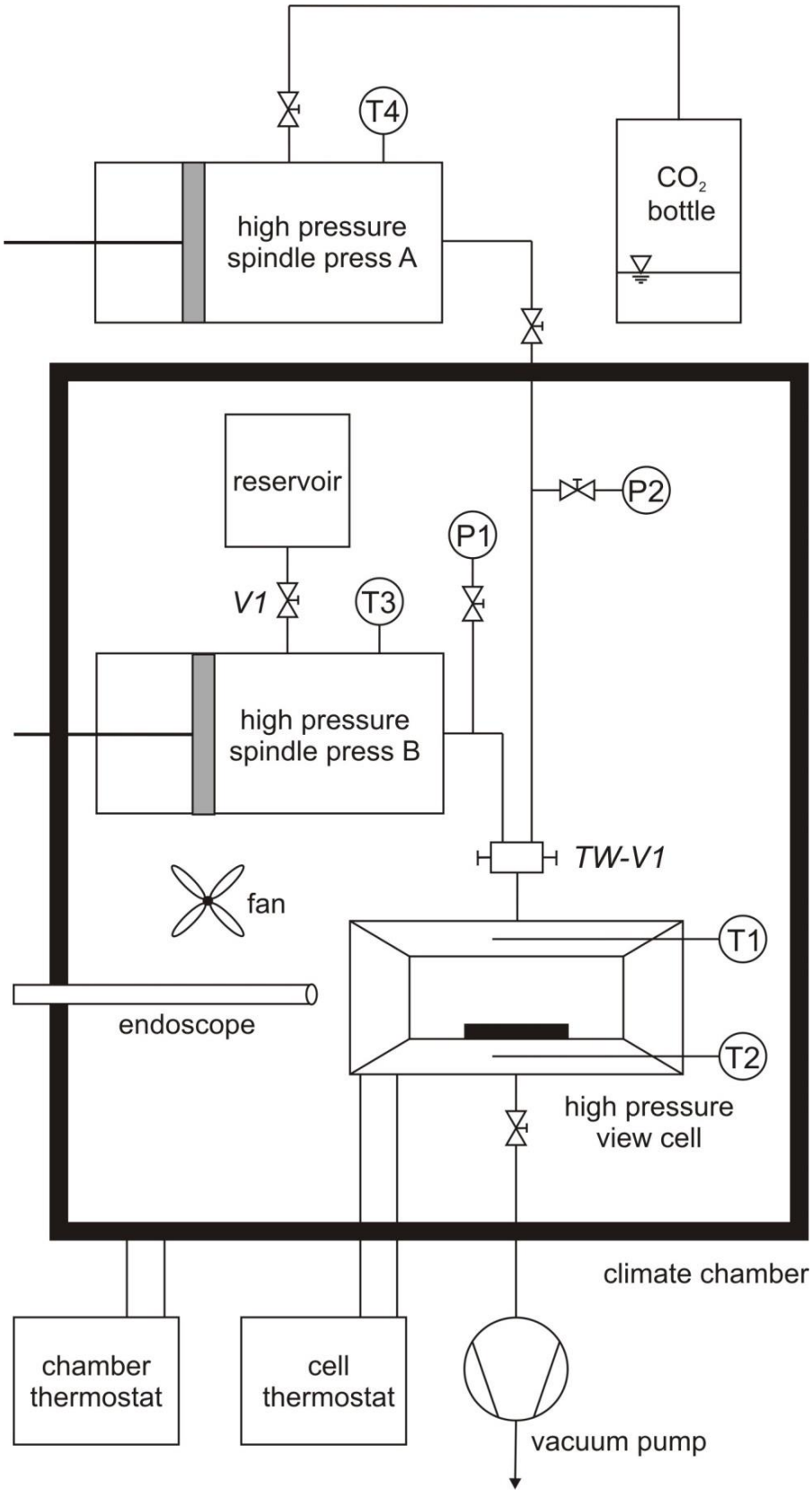
T4
high pressure
spindle press A
CO2
bottle
reservoir
P2
P1
V1
T3
high pressure
spindle press B
TW-V1
fan
T1
endoscope
T2
high pressure
view cell
climate chamber
chamber
thermostat
cell
thermostat
vacuum pump

Figure 3.

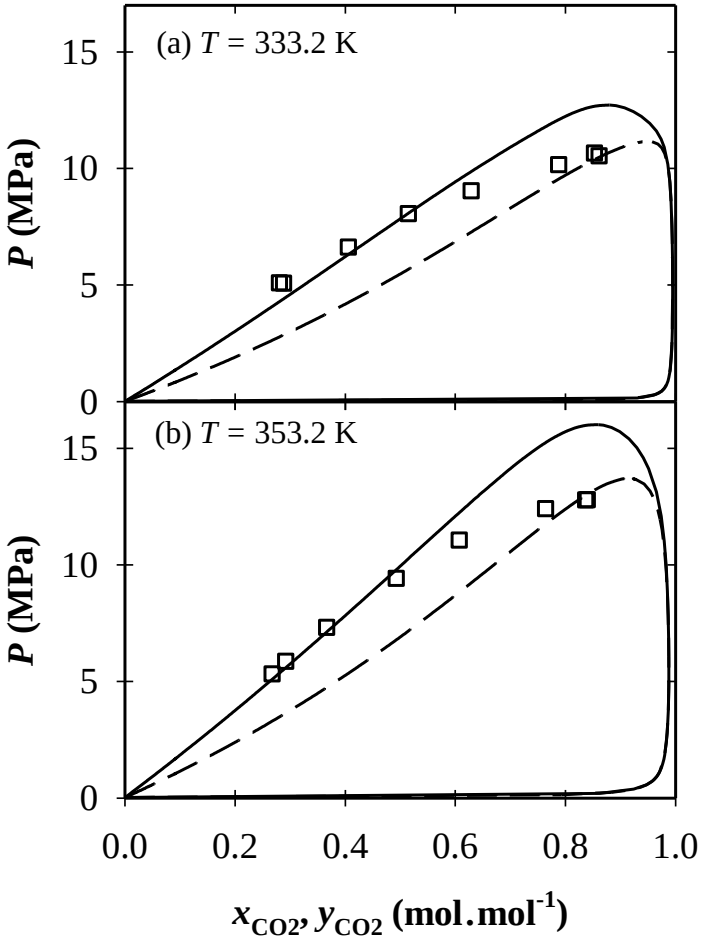
(a) T = 333.2 K
(b) T = 353.2 K
P (MPa)
P (MPa)
15
10
5
0
15
10
5
0
0.0
0.2
0.4
0.6
0.8
1.0
x_CO2, y_CO2 (mol.mol-1)

Figure 4.

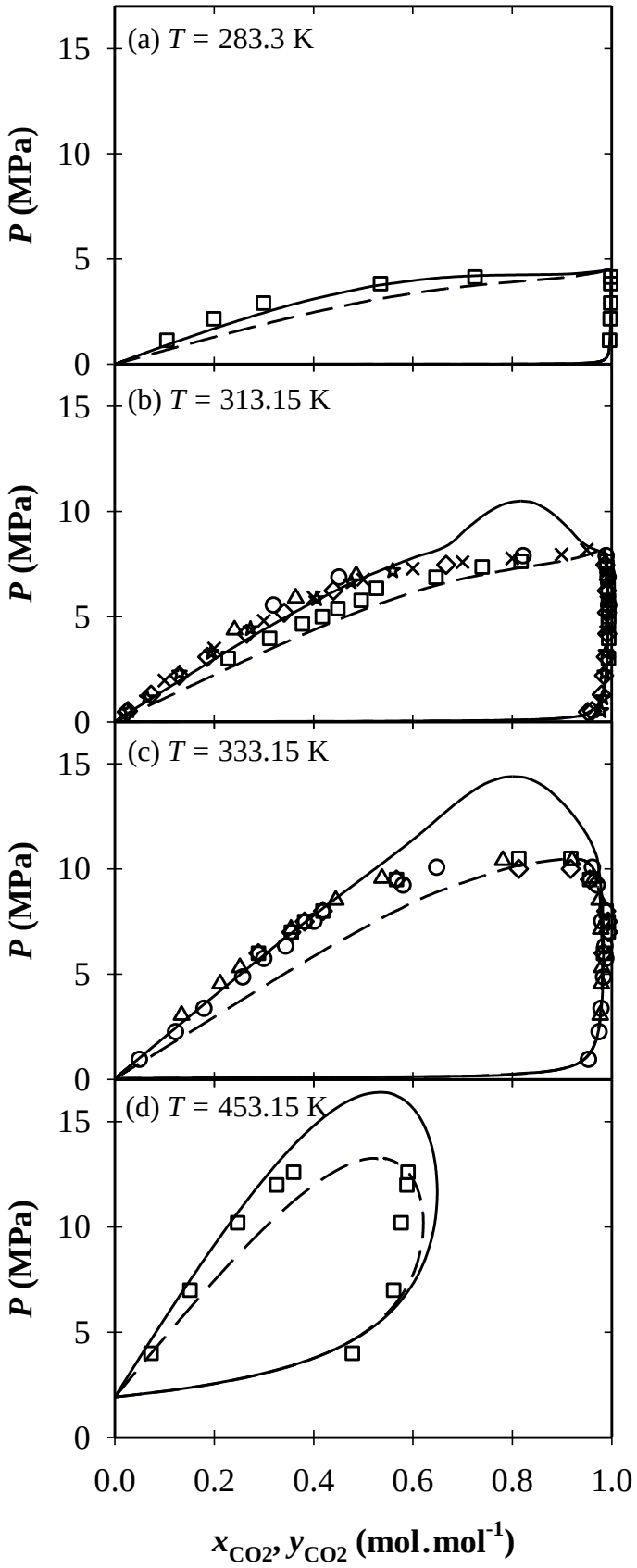
(a) T = 283.3 K
(b) T = 313.15 K
(c) T = 333.15 K
(d) T = 453.15 K
P (MPa)
0
5
10
15
0.0
0.2
0.4
0.6
0.8
1.0
x_CO2, y_CO2 (mol.mol-1)

Figure 5.

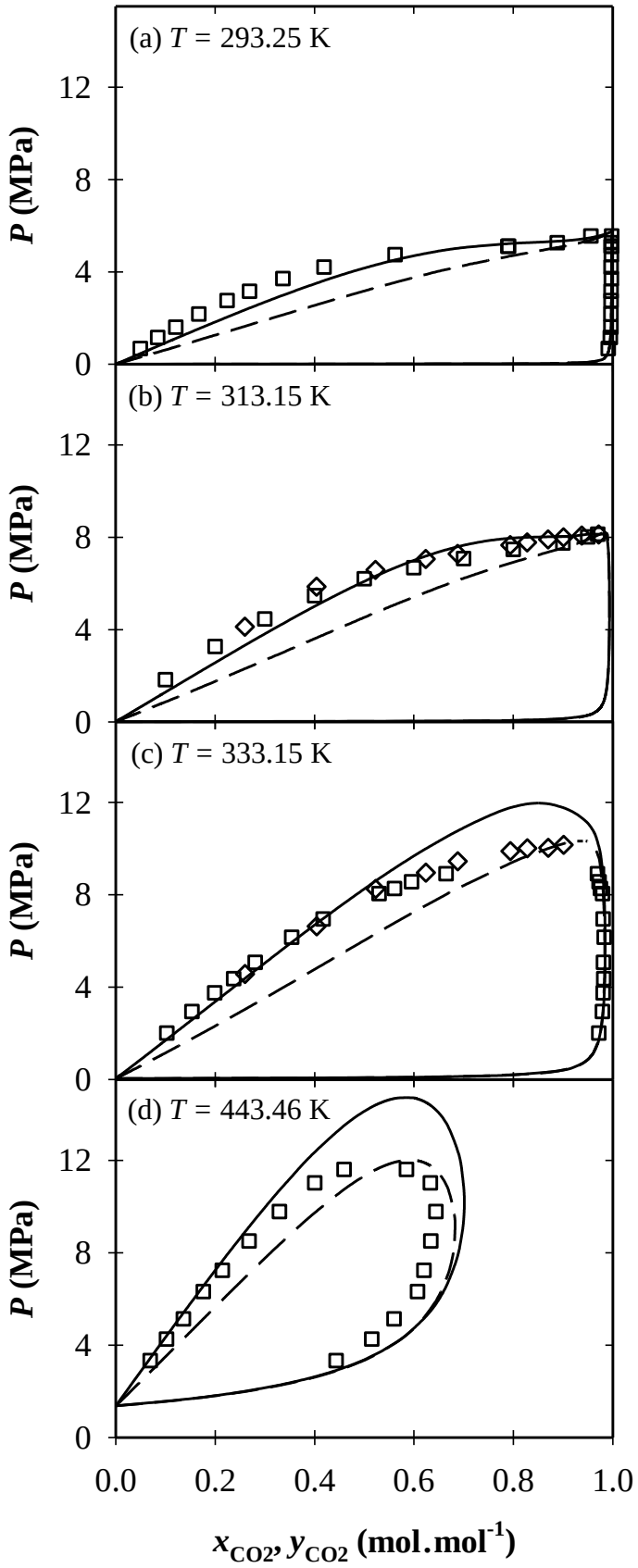
(a) T = 293.25 K
(b) T = 313.15 K
(c) T = 333.15 K
(d) T = 443.46 K
P (MPa)
0
4
8
12
0.0
0.2
0.4
0.6
0.8
1.0
x_CO2, y_CO2 (mol.mol-1)

Figure 6.

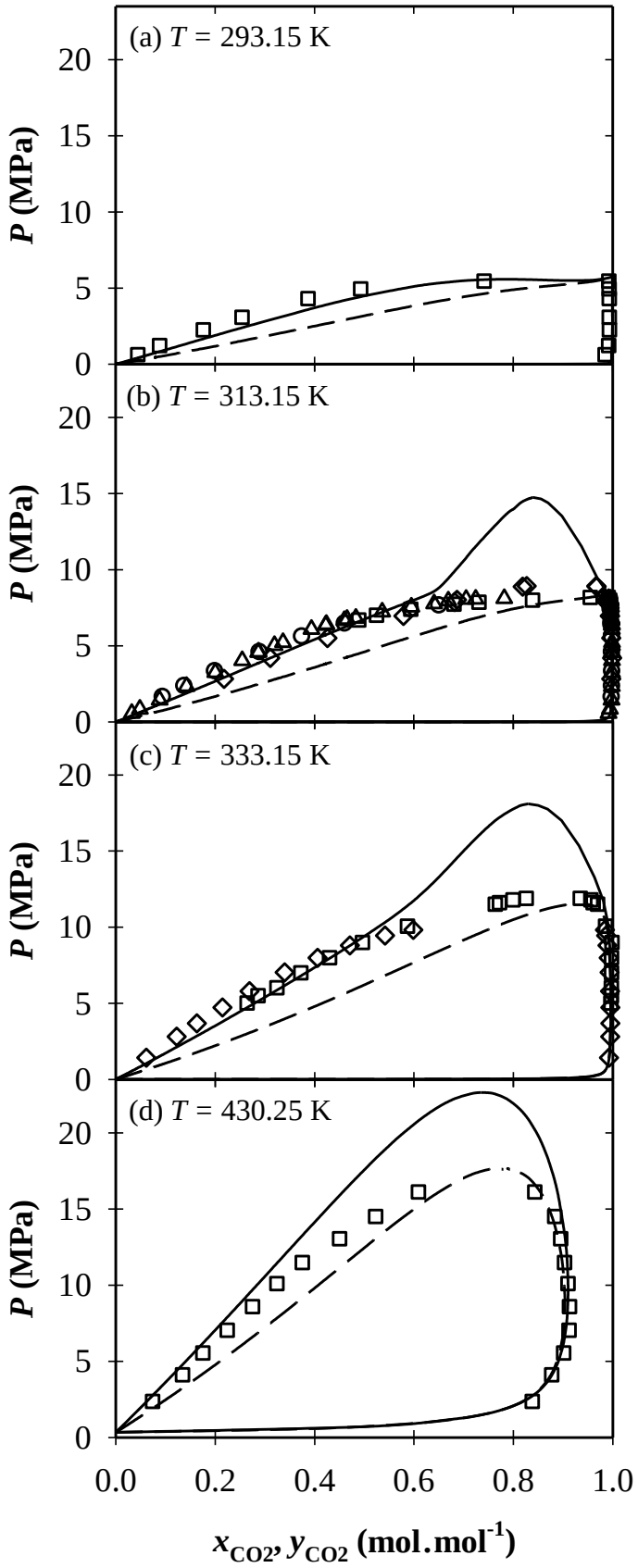
(a) T = 293.15 K
(b) T = 313.15 K
(c) T = 333.15 K
(d) T = 430.25 K
P (MPa)
0
5
10
15
20
0.0
0.2
0.4
0.6
0.8
1.0
x_CO2, y_CO2 (mol.mol-1)

Figure 7.

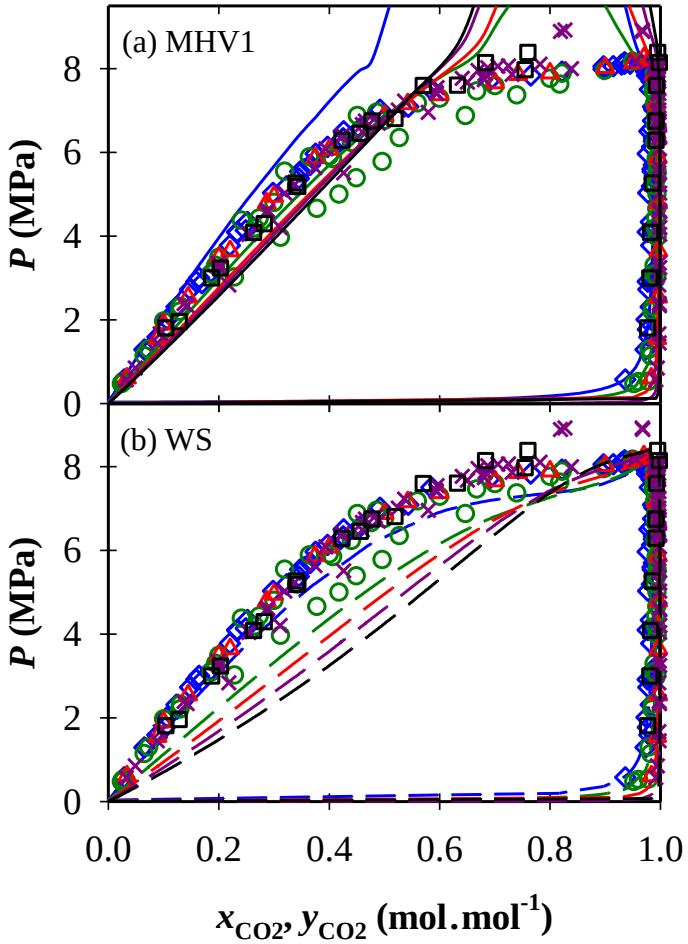

Figure 8.

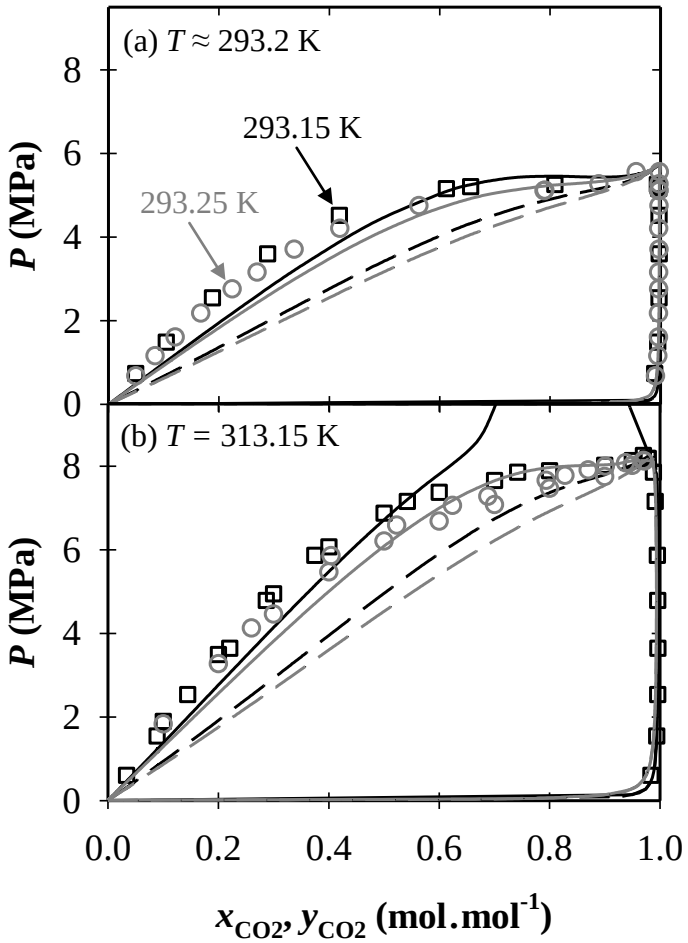
(a) T ≈ 293.2 K
293.15 K
293.25 K
P (MPa)
(b) T = 313.15 K
P (MPa)
0.0
0.2
0.4
0.6
0.8
1.0
x_CO2, y_CO2 (mol.mol-1)

Figure 9.

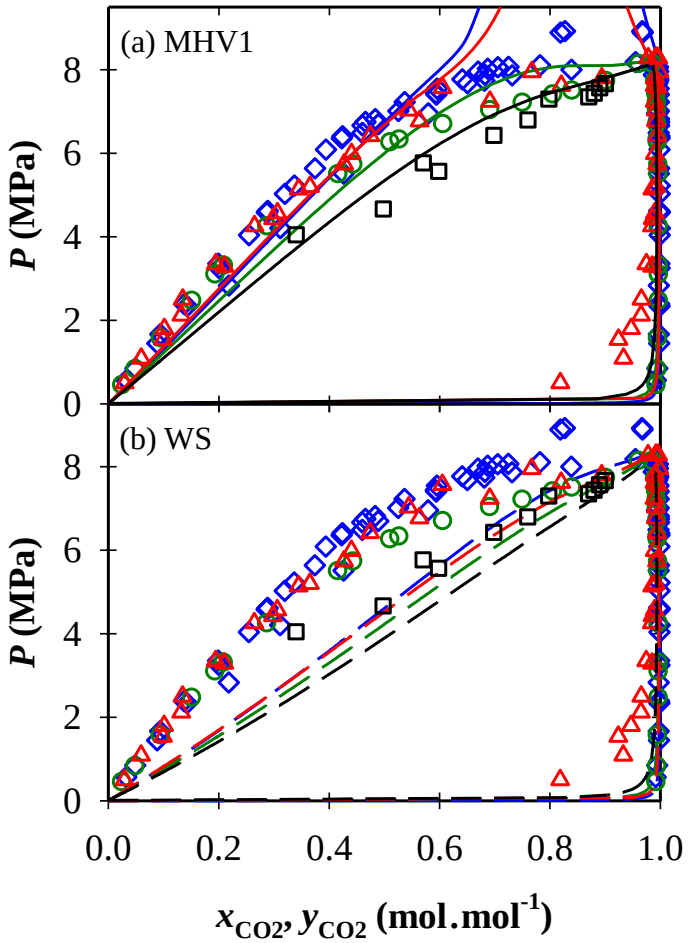

Figure 10.

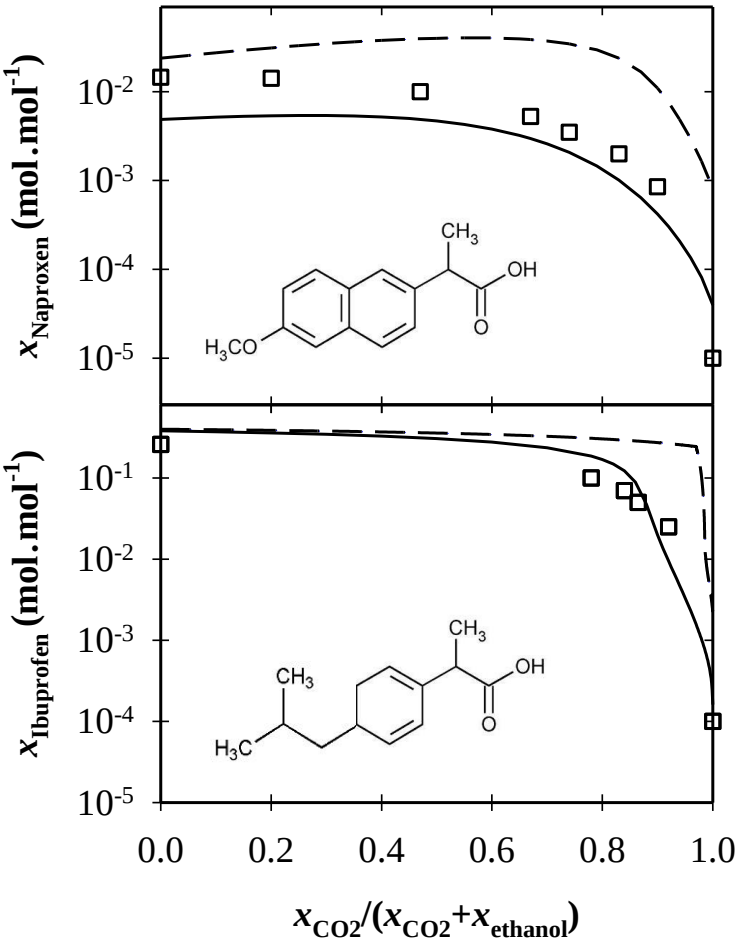
$x_{Naproxen}$ (mol.mol^{-1})
10^{-2}
10^{-3}
10^{-4}
10^{-5}
H_3CO
CH_3
OH
O
$x_{Ibuprofen}$ (mol.mol^{-1})
10^{-1}
10^{-2}
10^{-3}
10^{-4}
10^{-5}
H_3C
CH_3
CH_3
OH
O
0.0
0.2
0.4
0.6
0.8
1.0
$x_{CO2}/(x_{CO2}+x_{ethanol})$

TOC Graphic

of

Vapor-liquid equilibria of CO_2 + C1-C5 alcohols from experiment and the COSMO-SAC model

Chieh-Ming Hsieh*, Thorsten Windmann, Jadran Vrabec

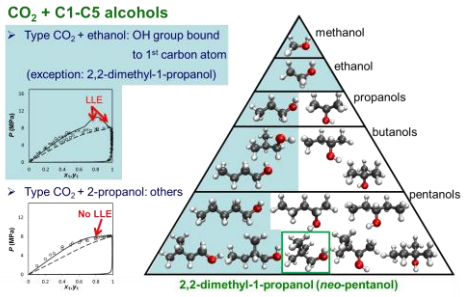

TOC Graphic: for Table of Contents use only